Science of the Total Environment 667 (2019) 325–337

Contents lists available at ScienceDirect

Science of the Total Environment

journal homepage: www.elsevier.com/locate/scitotenv

A flood susceptibility model at the national scale based on multicriteria analysis

Pedro Pinto Santos [a,*], Eusébio Reis [a], Susana Pereira [a], Mónica Santos [a,b]

[a] Centre for Geographical Studies of the Institute of Geography and Spatial Planning, University of Lisbon (CEG-IGOT-ULisboa), Edifício IGOT, Rua Branca Edmée Marques, Cidade Universitária, 1600-276 Lisboa, Portugal

[b] Centre for the Research and Technology of Agro-Environmental and Biological Sciences of the University of Trás-os-Montes and Alto Douro (CITAB-UTAD), Quinta de Prados, Ed. dos Blocos Laboratoriais Sala C1.10, 1° Piso, 5001-801 Vila Real, Portugal

HIGHLIGHTS

- Flow accumulation, slope and permeability are applied to assess stream flood susceptibility.
- Using the cumulative function assures that the entire basin is considered downstream.
- Model validation is done by correlation with >2200 historical flood cases.
- Results provide an accurate distinction of transboundary, regional and local rivers.
- Municipal profiles of flood susceptibility and flood cases are defined.

GRAPHICAL ABSTRACT

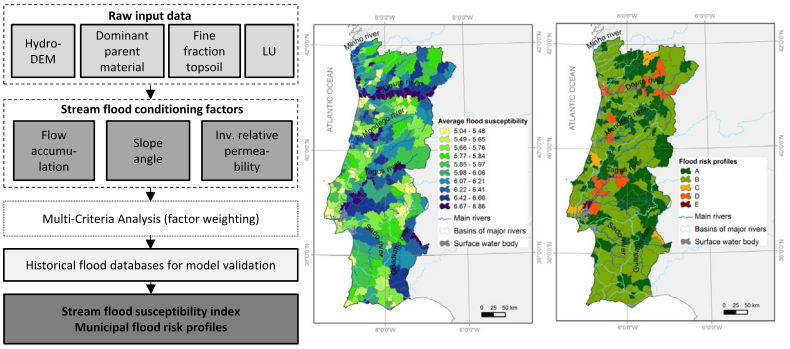

ARTICLE INFO

Article history:
Received 8 November 2018
Received in revised form 20 February 2019
Accepted 21 February 2019
Available online 23 February 2019

Editor: Ouyang Wei

Keywords:
Stream flood susceptibility
Conditioning factors
Flood databases
Flood risk profile

ABSTRACT

River flooding is a specific worldwide type of flooding responsible for considerable human and material losses. An extensive knowledge about flood conditioning factors and a diverse set of methodologies for flood susceptibility evaluations are available, although there is still field for improvement regarding methodologies for small-scale flood susceptibility assessment, particularly relevant in data-scarce contexts.

This research applied to mainland Portugal, introduces a multicriteria methodology to assess flood susceptibility at national scale considering three flood-conditioning factors: flow accumulation, average slope angle and average relative permeability. These three factors resume other factors usually considered in literature, related to morphology and potential runoff. This work includes data from the flood conditioning factors considering the cumulative role of the entire contributive area and not only the on-site characteristics. The weight of each factor was assigned based on expert opinion and validated using available flood damages databases with >150 years of records.

From the several tested flood susceptibility models, the one that best fits the historical records was chosen, which corresponds also to a more valued role of flow accumulation factor. Results provide an accurate differentiation of transboundary, regional and local rivers. The scores of stream flood susceptibility were later transformed to a single value per each of the 278 municipalities of mainland Portugal. Representing the natural susceptibility to river flooding, these results can be cross-analyzed with structural mitigation measures, spatial

* Corresponding author.
E-mail addresses: pmpsantos@campus.ul.pt (P.P. Santos), eusebioreis@campus.ul.pt (E. Reis), susana-pereira@campus.ul.pt (S. Pereira), monica.santos@utad.pt (M. Santos).

https://doi.org/10.1016/j.scitotenv.2019.02.328

planning instruments, exposure and vulnerability data along the respective floodplains, in order to identify water streams that require a more detailed and concerned future intervention and an exhaustive susceptibility study at the local scale.

1. Introduction

Decision-making processes require the continuous development of methodologies able to produce valuable information about flood susceptibility, in order to support most efficient flood risk management strategies. In this process, flood susceptibility assessment approaches that combine different methodologies – geomorphological, historical, hydrological and hydraulic – are particularly valuable (e.g. Benito et al., 2004; Santos et al., 2011; Garrote et al., 2017; Wing et al., 2018), as well as those that rely on high-resolution digital elevation models (DEMs) (e.g. Vojtek and Vojteková, 2016) as a decisive factor to compute flood-prone areas (Casas et al., 2006), regardless of procedures that might contribute to reduce the need of such detailed DEMs (Saksena and Merwade, 2015).

However, constraints on time and data availability – high-resolution DEMs, permeability-related data, rainfall-runoff data or historical records, for example – or the need to assess flood hazard homogeneously on large areas, prevent researchers from applying such complex and detailed methods. In the so-called data scarce contexts, the application of coupled methodologies is quite often not possible, requiring the search for more expedite approaches (Hagen et al., 2010; Vahid et al., 2018). On these approaches, the widespread of remote sensing-derived products (for elevation, rainfall, land use or permeability data, among others) in recent years made possible the development of a diverse set of multicriteria methods to assess flood susceptibility, with the capacity of being applied to vast areas, at country or regional level. In the flood susceptibility assessment, the identification and selection of flood conditioning factors, their correlations and multicollinearity are fundamental to retain only the more relevant and independent ones. Multicriteria methods strongly rely on geomorphic and geomorphic-derived variables, but also uses other conditioning factors related to rainfall (annual amount and intensity) and permeability (inferred from soil, geological and land use data) (Kourgialas and Karatzas, 2011; Tehrany et al., 2015; Vahid et al., 2018).

The set of available algorithms for assessing the role of each factor, or class inside the factor, is diverse and includes, not exclusive to, support vector machine (e.g. Tehrany et al., 2015), analytic hierarchical process (e.g. Yang et al., 2013; Kazakis et al., 2015), weights-of-evidence (Tehrany et al., 2014; Rahmati et al., 2016), frequency ratio (Lee et al., 2012; Rahmati et al., 2016), fuzzy inference (Hong et al., 2018; Razavi Termeh et al., 2018) or logistic regression (Pradhan, 2009). The use of training and validation datasets of past floods is widely used, evidencing the relevance of adequately collecting and integrating flood historical databases.

The scale of the study areas where multicriteria methods have been applied is quite diverse. There are examples at the city level (Lee et al., 2012), at the basin and district level (Manfreda et al., 2014; Kazakis et al., 2015; Tehrany et al., 2015; Vahid et al., 2018), and at the province and country-level (Rahmati et al., 2016; Cunha et al., 2017; Kourgialas and Karatzas, 2017; Zhao et al., 2018).

In this context, the main objective of this research is to assess stream flood susceptibility at the national level. In order to achieve this goal, flood conditioning factors and their integration representing the propensity of the river network to generate floods will be assessed. The applied method for assessing flood susceptibility performs the evaluation of drainage area conditions for each point in the river basin. This is done by considering the cumulative function of the conditioning factors (area flow, slope and relative permeability). The innovative contribution of this work is to provide a comparable nation-wide evaluation of streams' susceptibility to flooding, incorporating data from the entire contributive areas and not only from the on-site characteristics of streams. A multicriteria approach to assess flood susceptibility was applied in Portugal, at the local scale to a sub-basin of 979 km^2 (Santos and Reis, 2018) and to the entire mainland Portugal (≈89,000 km^2) by Jacinto et al. (2015). However, this later national-scale study differs in two aspects from the presented research: it used two distinct flood conditioning factors — cost distance (based on the hydrographic network and the slope) and flow number (CN) without considering the whole contributing area of the transboundary rivers; and the goal to identify flood-prone areas. Apart from these two methodologically close studies, there is a research gap, not only in Portugal, regarding the evaluation of the susceptibility of streams to flooding.

After assessing national susceptibility on a cell-by-cell basis, a municipal representation of stream flood susceptibility was done, which allows to hierarchize the flood susceptibility at the national level and to be cross-analyzed with exposure and vulnerability data in the support of the definition of flood risk management strategies.

2. Study area

The basins of the main rivers that drain into mainland Portugal have their headwaters in Spain: Minho basin (17,080 km^2), Douro basin (97,478 km^2), Tagus basin (80,500 km^2) and the Guadiana basin (67,000 km^2) (Fig. 1). The river regime is determined by the pluvial regime. The snow accumulation, although not dominant for the river regime, may have some contribution to river flow, particularly on the transboundary basins (e.g. Diéz-Herrero et al., 2013).

In mainland Portugal, elevation ranges from 0 to 1993 m a.s.l. The morphology of the area extending north of the Tagus valley is dominated by mountains, plateaus and incised valleys defined by steep slopes. In contrast, vast plains and hilly relief generally mark the southern half of the country. According to the Köppen-Geiger-Pohl climate zones' classification, two main types of the Mediterranean climates (Cs) are found in the country: Csb on the north and Csa, generally on the southern part of the Portuguese territory. In terms of rainfall, Cs climates are defined by total rainfall lower than 40 mm on the driest month (summer); and the wettest month is found on the winter season, which records a total rainfall at least 3 times higher than in the driest month. Up to 50% of the total rainfall on winter (D-J-F months) is due to cyclonic and directional W and SW atmospheric rivers (Ramos et al., 2014). During the summer months rainfall is usually associated with N and E flows, although local factors such as relief and deep convective depressions are relevant in conditioning the spatial variability of intense rainfall events (Ramos et al., 2014). Rainfall amount in summer is residual, about 6% of the annual amount (de Lima et al., 2015). According to the same study, spring and autumn rainfall is mainly due to W circulation and cyclonic conditions. Spring and autumn months are transitional months and total rainfall can vary significantly (Gallego et al., 2011; Miranda et al., 2002; Trigo and Dacamara, 2000).

From the above context and according to the DISASTER database (Zêzere et al., 2014), slow-onset floods are more frequent from November to February, although it may also occur on spring and autumn. Flash floods, however, may occur in any time of the year, although they are more frequent during the autumn and winter. Some of the Portuguese major cities with the highest resident population (e.g. Porto, Aveiro, Coimbra, Santarém, Lisbon and Setúbal) are bathed by the main rivers (Fig. 1).

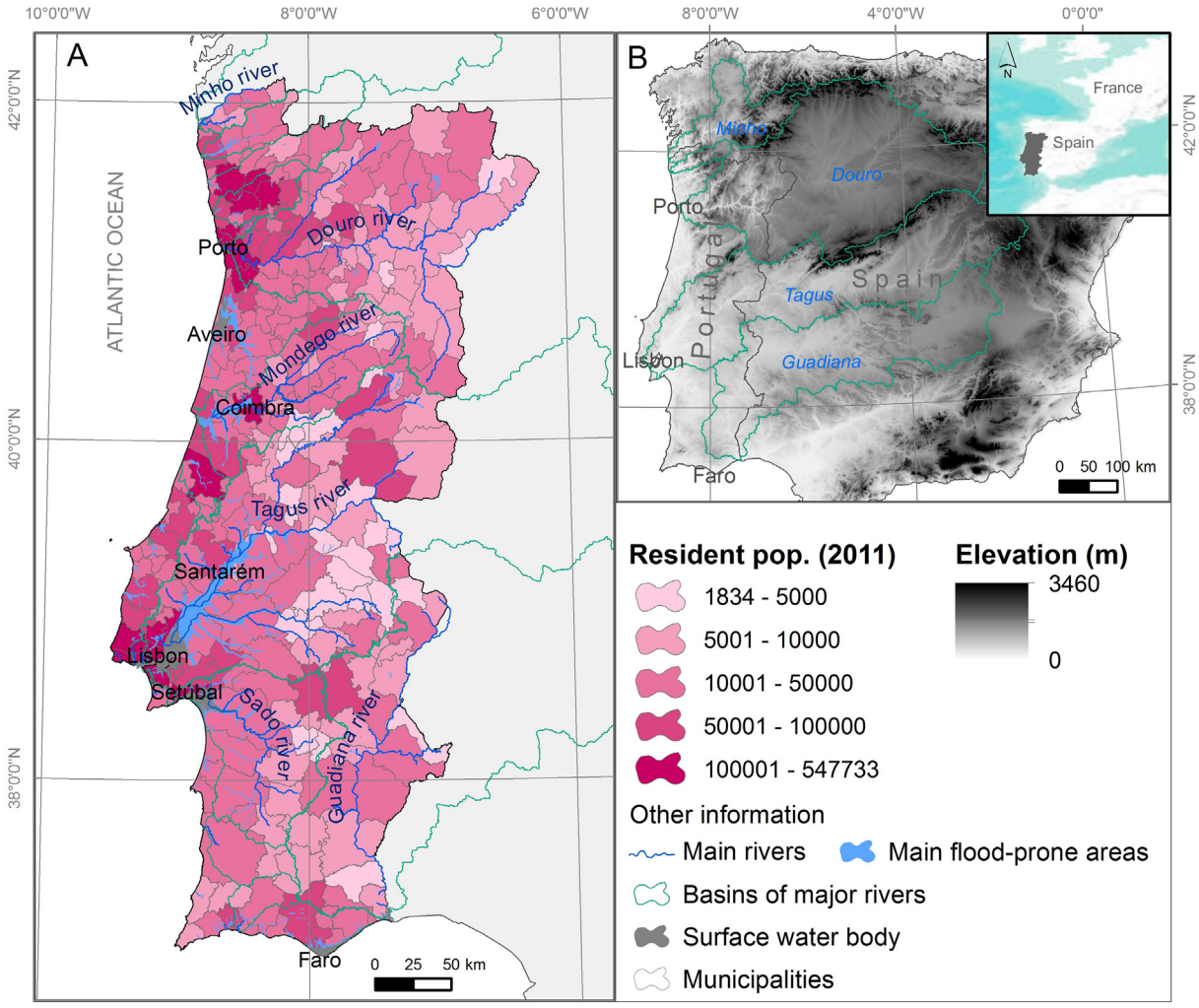

Fig. 1. Resident population (2011) per municipality in mainland Portugal (A) and elevation in Iberian Peninsula (B).

3. Data and methods

Stream flood susceptibility was assessed following a multicriteria analysis approach, in which the characterization of the river dynamics along the drainage network is obtained by the iterative definition of the weight of each conditioning factor (Reis, 2011).

Three stream flood conditioning factors were used: flow accumulation, average slope angle and average inverse relative permeability (Fig. 2). Although the objective of the research is to assess stream flood susceptibility for mainland Portugal, conditioning factors were collected for the entire contributing areas that drain to mainland Portugal, considering the Spanish part of the transboundary basins. This procedure is necessary because the cumulative role of the entire drainage areas must be accounted for the definition of the local conditions on downstream areas. Based on the DEM (see Section 3.1), each terrain unit is represented by a cell of 3 arc-second size (≈86.5 m).

After applying the accumulation and average functions, the values of the three flood conditioning factors were transformed into their natural logarithms because the distribution of raw data was strongly asymmetric, positively skewed, in particular in regard to the flow accumulation and average slope. This extreme asymmetry was affecting the final susceptibility maps, after applying weights, to be scored equally on slopes and streams, particularly on small and medium basins. The susceptibility scores result from the sum of weighted linear combinations of the three conditioning factors (Kourgialas and Karatzas, 2011). The three models that resulted from the tested combination of weights were correlated with damaging floods historical records (cf. Section 3.4) in order to support the selection of the best model, which, after classification, results on the final map of stream flood susceptibility. The final output expresses the susceptibility of streams to enter in flooding conditions, i.e., a classification of the river network is obtained according to the capacity to generate floods (Reis, 2011). Finally, an average score of stream flood susceptibility is calculated per municipality in order to hierarchize the 278 municipalities of mainland Portugal.

3.1. DEM derived data

3.1.1. Flow accumulation

Flow accumulation (F_{acc}) was calculated from the Shuttle Radar Topography Mission (SRTM) DEM for the entire Iberian Peninsula with a 3 arc-second resolution, downloaded from the CGIAR-CSI mirror service (http://srtm.csi.cgiar.org/). Flow direction was calculated from the hydrologically corrected DEM. Finally, the flow accumulation function of the ArcGIS Spatial Analyst® extension was used to obtain F_{acc}, clipped to mainland Portugal boundaries. The result range from 1 to 13,029,779 cells (each cell represents about 7482 m^2, so the highest value corresponds to 97,489 km^2), to which the natural logarithm was applied, resulting in a range from 0 to 16.38. In order to apply the weights uniformly between the three conditioning factors, F_{acc} values

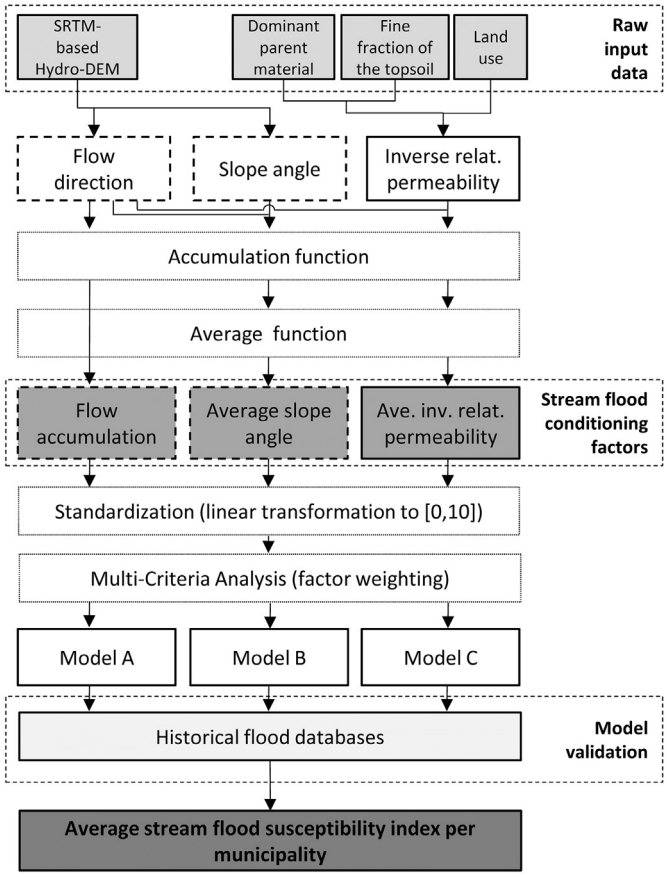

Fig. 2. Methodological scheme for the national scale stream flood susceptibility assessment.

were linearly transformed to the range [0, 10] using the function $y = 0.61x$, in which x represents the number of accumulated cells.

3.1.2. Average slope angle

Slope angle in degrees was calculated using the hydrologically corrected SRTM-based DEM for the entire Iberian Peninsula in the GIS extension ArcGIS Spatial Analyst®. Within the same GIS tool, flow accumulation was ran using as input the previously obtained flow direction raster dataset and using as weight factor of the slope angle raster dataset (S), which results in the accumulated slope angle (S_{acc}). Average slope angle (S_{avg}) is obtained by dividing accumulated slope by flow accumulation and clipping the raster dataset to mainland Portugal.

As performed with F_{acc}, the natural logarithm was applied to the average slope raster dataset, resulting in scores ranging from [−6.3, 3.7]. The final raster dataset of average slope angle (S_{avg}) is the result of the transformation of those scores to the interval [0, 10] using the linear function $y = x + 6.3$.

3.2. Average inverse relative permeability

Relative permeability was estimated using three data sources: dominant parent material (*DPM*), fine fraction of the topsoil (*FFT*) and land use (*LU*). *DPM* and *FFT* express the natural permeability, while *LU* represents the effect of the land use coverage on infiltration. Initially, data was prepared and processed on the perspective that high scores mean high permeability. Only after obtaining a final score of relative permeability the scores were inverted in order that higher values contribute to higher flood susceptibility and vice-versa. All three input data covered the entire area of the transboundary basins that drain to mainland Portugal.

Table 1
Dominant parent material classes and respective *DPM* scores.

DPM code	*DPM* legend (3rd level)	*DPM* score
0	No information	1
100	Consolidated-clastic-sedimentary rocks	6
121	Sandstone	5
122	Arkose	5
131	Claystone/mudstone	2
211	Limestone	7
214	Marl	5
310	Acid to intermediate plutonic rocks	3
311	Granite	3
313	Diorite	3
321	Gabbro	4
411	(Meta-)shale/argilite	2
420	Acid regional metamorphic rocks	3
510	Marine and estuarine sands	8
520	Marine and estuarine clays and silts	1
531	River terrace sand or gravel	9
540	Fluvial clays, silts and loams	1
550	Lake deposits	1
720	Eolian sands	10
800	Organic materials	6

3.2.1. Dominant parent material

The third level of the dominant parent material (*DPM*) European-level cartography was used. This data represents the lithological substrate beneath the soil layer and is available at the European Soil Data Centre (ESDAC) (Panagos et al., 2012), from which a score of the relative infiltration of *DPM* was assigned (minimum value is 1 and maximum value is 10) (Table 1).

3.2.2. Fine fraction of the topsoil

The fine fraction of the topsoil (*FFT*) was estimated based on the LUCAS top soil characteristics (Ballabio et al., 2016) available at the ESDAC of the European Commission's Joint Research Centre (Panagos et al., 2012). This dataset is available as a raster dataset with a resolution of 500 m. The results considered that the percentage of fine fraction is the sum of the total percentage of clay (<0.002 mm) and silt (0.002–0.05 mm) and 5% of sand (0.05–2.0 mm). This sum is then divided by the total soil composition (clay, silt, sand and coarse material (>2 mm)), resulting in a proportion of fine fraction ranging from 0 to 1. These values were classified in 10 classes of equal intervals ranging between 1 and 10 (e.g. *FFT* between 0 and 0.1 is classified as 1) to keep the consistency of the classification between 0 and 10 used on the other flood susceptibility conditioning factors. Inverse distance weight (IDW) interpolation was applied to the points extracted from the classified *FFT* raster dataset in order to resize the original resolution

Table 2
Corine Land Cover classes and their effect score on infiltration.

Classes of Corine Land Cover 2012	*LU* effect score on infiltration
111 Continuous urban fabric	0.0
112 Discontinuous urban fabric	0.5
121 Industrial or commercial units	0.0
122 Road and rail networks and associated land	0.4
123 Port areas	0.0
124 Airports	0.4
131 Mineral extraction sites	1.0
132 Dump sites	0.0
133 Construction sites	0.3
141 Green urban areas	0.5
142 Sport and leisure facilities	0.2
2 Agricultural areas	1.0
3 Forest and semi natural areas	1.0
4 Wetlands	0.0
5 Water bodies	0.0

to match the 3 arc-second resolution used on the other conditioning factors, built with the SRTM-based DEM.

3.2.3. Land use

The Corine Land Cover 2012 (CLC2012) dataset (EEA, 2012) was used to estimate the effect of land use (*LU*) on the soil and lithological permeability. The scores assigned to *LU* classes represent the fraction – between 0 and 1 – of the available rainfall to runoff on each CLC2012 class (Table 2). A score of 0 is applied to impervious areas and means the highest availability of rainwater to runoff. Where land use is not interfering with natural infiltration a score of 1 is assigned.

3.2.4. Relative permeability

After obtaining the three input data (Fig. 3) used to describe relative permeability (P_{rel}) – dominant parent material (*DPM*), fine fraction of the topsoil (*FFT*) and land use (*LU*) – the respective raster datasets were combined as described on Eq. (1):

$$P_{rel} = \frac{(DPM + FFT)}{2} \cdot LU \quad (1)$$

Secondly, $Prel_{inv}$ was calculated by inverting the scores of P_{rel} so that higher values correspond to higher contribution to increase flood susceptibility.

Similarly, to the other flood conditioning factors, the flow accumulation tool of the ArcGIS Spatial Analyst® extension was used to obtain the accumulated inverse relative permeability, in which flow direction is used as input data and the inverse relative permeability ($Prel_{inv}$) as the weight factor ($Prel\_inv_{acc}$). The scores were divided by F_{acc} to obtain the average inverse relative permeability ($Prel\_inv_{avg}$). The natural logarithm was applied to these scores in order to obtain new values ranging from [−1.2, 2.3] which were transformed to the interval [0, 10] using the linear function $y = 2.9x + 3.4$.

3.3. Historical flood databases

Historical flood databases such as the DISASTER database (Zêzere et al., 2014) and other flood documental databases, both based on newspapers (Santos et al., 2018; Santos and Reis, 2018) were used to select the best combination of flood conditioning factors' weights and to further validate the flood susceptibility model at the stream network. In Portugal, there is a lack of consistent flood databases in spatial and temporal terms in the southern region of the country, which prevented the selection of this region for validation purposes.

In both databases, those flood cases classified as 'urban floods' or 'other type of floods' were excluded from this analysis. Also, only flood cases with georeferencing accuracy were used (e.g. based on the exact coordinates, approximated by toponymy or by descriptions and morphology).

The DISASTER database includes 932 flood DISASTER cases that generated human losses (1 or more casualties, missing, injured, displaced or evacuated persons), in mainland Portugal, for the period 1865–2015. The other flood documental databases complement the DISASTER database by adding the flood cases in which only minor losses are reported (i.e., not the human-type losses described in regard to the DISASTER database). This database of minor flood cases was compiled for specific study areas (Fig. 4). The North flood database (Santos et al., 2018), includes 1301 flood cases (319 of them from the DISASTER database) for the period 1865–2016. Two subsets were selected from the North database, corresponding to the Lima and the Tâmega River basins. The Lima River basin, located in a granitic area, includes 147 flood cases (22 of them from the DISASTER database). The Tâmega River basin is located in a predominant metasedimentary and granitic geological context and includes 114 flood cases (28 of them from DISASTER database). In the Central region of Portugal, another river basin flood database was used, the Águeda River basin (Santos and Reis, 2018), which is located in a geological transition between schists and greywackes of the Hesperian Massif (East) and the detrital formations of the Mesocenozoic (West), including 322 flood cases (16 of them from the DISASTER database) for the period 1935–2010.

At the national level, the distribution of damaging flood cases is clearly associated with the major rivers' floodplains and of the urban settlements' location (mainly, the largest cities of Porto, Coimbra and Lisbon) (Fig. 4A). The majority of the sparsely distributed points located south of the Tagus River are flood cases caused by flash floods. On the North, the distribution of flood cases follows generally that same pattern: a concentration of flood cases along the major river (the Douro) and on the low-lying and more urbanized areas, that are located generally on a stretch of 50 km from the shoreline.

On the Lima basin, flood cases concentrate along the major and homonymous river, particularly on the last 50 km of its course to the sea (downstream of the city of Ponte de Lima), although some flood cases are also found on the upper sectors of minor streams. On the Tâmega basin, flood cases concentrate on two sectors: an upper sector near the city of Chaves; and a lower sector, along a reach of 30 km length between the city of Amarante and the downstream confluence with the Douro River. As mentioned, the Águeda basin presents two distinct hydrological features. The eastern sector of the basin, less populated but more impervious, generates flooding on the low-lying agricultural

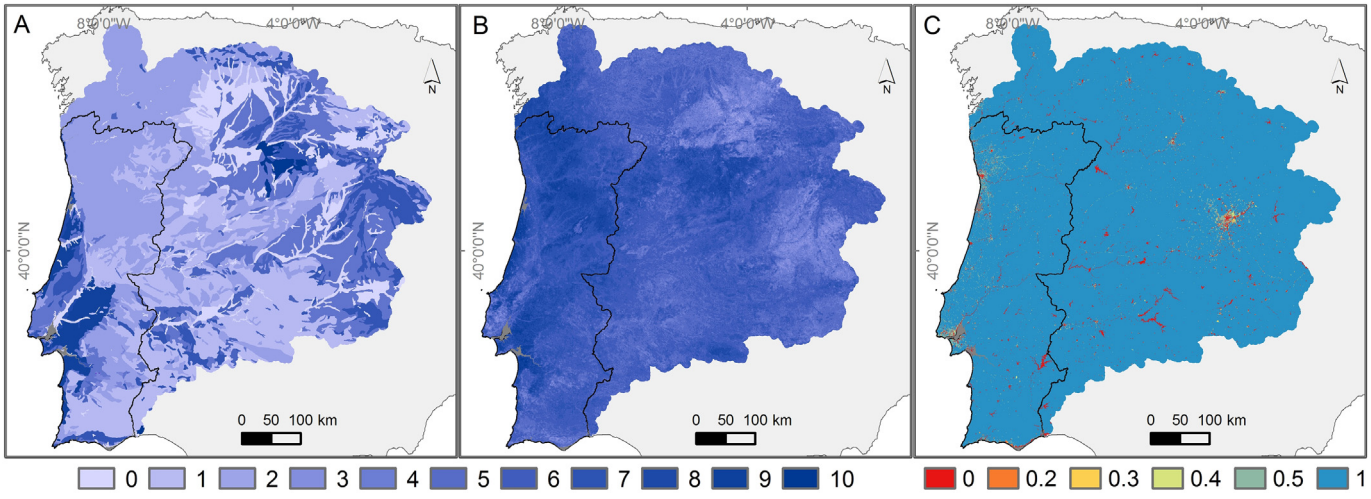

Fig. 3. Scores assigned to the three input data used on the assessment of relative permeability: dominant parent material (A), fine fraction of the topsoil (B) and land use (C).

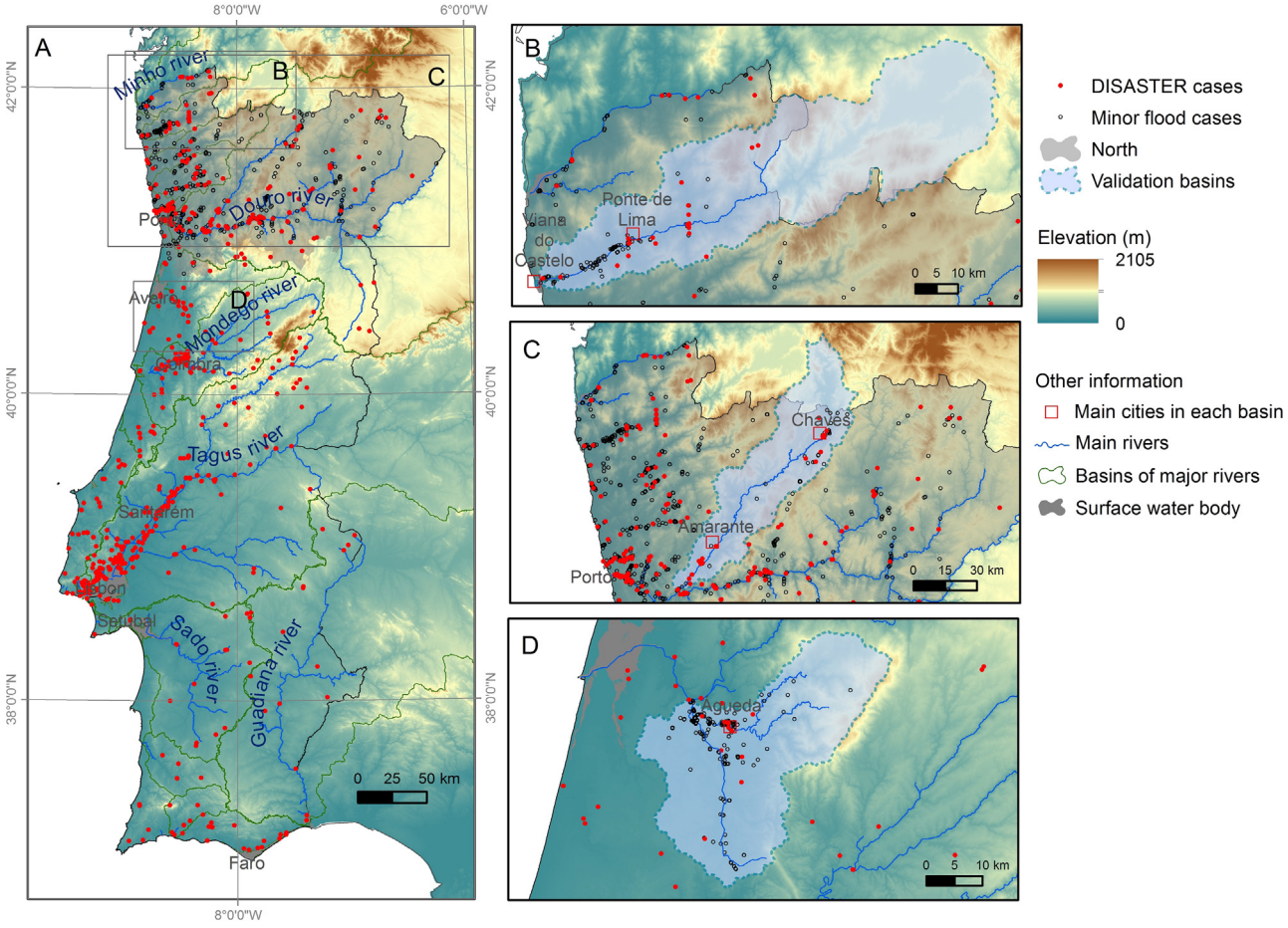

Fig. 4. Historical flood records of Disaster and North databases (A), and Lima (B), Tâmega (C) and Águeda (D) basins.

areas and the city of Águeda. The western sector, more urbanized, causes floods of minor consequences but more evenly distributed throughout the sub-basin's area, even near the headwaters, which does not occur on the eastern sector (Fig. 4D).

3.4. Factor weighting and model validation

The final index of stream flood susceptibility (*SFS*) was computed as follows (Eq. (2)):

$$SFS = F_{acc} * w_{F_{acc}} + S_{avg} * w_{S_{avg}} + Prel\_inv_{avg} * w_{Prel\_inv_{avg}} \quad (2)$$

Based on previous applications of this methodological approach in weighting flood conditioning factors through this methodology (Jacinto et al., 2014; Santos and Reis, 2018), the following three models were tested at the national scale:

1) Model A, with $w_{Facc} = 0.75$, $w_{Savg} = 0.15$ and $w_{Prel\_inv\_avg} = 0.10$;
2) Model B, with $w_{Facc} = 0.80$, $w_{Savg} = 0.10$ and $w_{Prel\_inv\_avg} = 0.10$;
3) Model C, with $w_{Facc} = 0.85$, $w_{Savg} = 0.10$ and $w_{Prel\_inv\_avg} = 0.05$.

The *SFS* scores range between 0 and 10. Values lower than 5 were excluded since they represent slopes, hilltops and small streams, where the physical conditions for flooding are quite low or inexistent. The remaining scores of the different models were classified equally in 5 classes: very low (VL, [5, 6]), low (L, [6, 7]), moderate (M, [7, 8]), high (H, [8, 9]) and very high (VH, [9, 10]) to allow the comparison of models' results.

Since the models classify the stream network susceptibility, the validation points from the historical flood databases were associated to the nearest streamline resulting from each model, instead of being associated to the value of the cell where are positioned. A spatial join between the *SFS* scores classified in 5 equal classes of each model and the datasets of flood cases (mainland Portugal, North and the three considered basins) was performed in ArcGIS® in order to obtain the nearest *SFS* class of each flood case.

The similarity between the spatial patterns of *SFS* in each of the three models was evaluated with the Kappa statistics, using the Map Comparison Kit software (MCK) (Visser and De Nijs, 2006). The MCK calculates the Kappa statistic (Cohen, 1960), a measure of similarity between two data sets or maps, representing the degree at which two distributions are equality located (Kappa location) or distributed (Kappa histogram), thus ranging from 0 to 1, where 1 means absolute similarity and 0 no spatial agreement. The Kappa index combines the two metrics by their product. According to Landis and Koch (1977), the spatial agreement expressed by the Kappa index can be interpreted as follows: poor (<0), slight (0–0.20), fair (0.21–0.40), moderate (0.41–0.60), substantial (0.61–0.80), and almost perfect (0.81–1.00).

Pearson correlation coefficients were calculated between the i) number of cells in each *SFS* class correlated with the number of flood cases per cell (P1) and ii) class of *SFS* (from very low to very high) correlated with the number of flood cases per cell in each *SFS* class (P2). For P1-type correlation coefficients, the more negative the correlation the better the model: in fact, the strongest association between flood occurrences and susceptibility occurs when high densities of flood cases occur in a small number of cells of high susceptibility. For P2-type coefficient correlations, the more positive the correlation the better the model because the highest densities of flood cases are expected to occur on the highest susceptibility classes. The correlations were calculated for the entire mainland Portugal (using only

DISASTER flood cases), and for the study areas described on Section 3.4 (North, Lima River basin, Tâmega River basin and Águeda River basin). The model selected as expressing stream flood susceptibility was the model that presented the strongest P1 and P2-type correlation coefficients on the study areas used for validation.

3.5. Municipal stream flood susceptibility and municipal risk profiles

Finally, an average value of *SFS* for each of the 278 municipalities in mainland Portugal was calculated using the *SFS* scores of the selected model. The same interval classes of the *SFS* were used. A cross-analysis of the average *SFS* and the historical DISASTER flood cases led to the definition of municipal profiles of flood risk in order to support decision-making in flood risk management.

4. Results

4.1. Stream flood conditioning factors and stream flood susceptibility models

Flow accumulation (F_{acc}), average slope angle (S_{avg}) and the average inverse relative permeability ($Prel\_inv_{avg}$) for mainland Portugal, linearly transformed to the interval [0, 10] are presented on Fig. 5. Highest values of F_{acc} are found along the major transboundary rivers (Douro, Tagus and Guadiana) since this factor is intrinsically related to the basins' area. S_{avg} is lower on floodplains, sand dunes and, generally, south of the Tagus River. $Prel\_inv_{avg}$ is higher on the areas where occurs an overlay of alluvial deposits, metamorphic and eruptive rocks, with high percentage of fine fraction soils, overlaid with artificialized areas. On the other hand, the relative permeability is higher on the low-lying sedimentary formations of the Vouga, Mondego, Tagus and Sado basins. Since the method aims at assessing the susceptibility of streams to the occurrence of flooding, the highest values of S_{avg} are associated with higher *SFS* due to the reduced concentration time or the reduced flow velocity along the basin (Fig. 5B).

In general, models B and C present the higher similarities as expressed by the Kappa index (Table 4). Between these two models, absolute similarity (Kappa = 1) is found on the high and very high classes of *SFS* regarding Kappa location. Models B and C keep the average slope weight as 0.1, reducing the weight of permeability and increasing the weight of flow accumulation. Accordingly, models A and C present themselves as the less similar in all the *SFS* classes in both Kappa location, histogram and index (Table 3).

Table 3
Kappa statistics for the paired-comparison for the three models of *SFS* (model A, B and C).

Kappa statistics on each *SFS* model	*SFS* classes				
	Very low [5, 6]	Low [6, 7]	Moderate [7, 8]	High [8, 9]	Very high [9, 10]
Model A versus model B					
Kappa location	1	0.93639	0.97067	0.9052	1
Kappa histogram	0.88515	0.88817	0.93807	0.97191	1
Kappa index	0.88515	0.83168	0.91056	0.87977	1
Model B versus model C					
Kappa location	0.9968	0.94498	0.97783	1	1
Kappa histogram	0.89657	0.89573	0.95940	0.94766	1
Kappa index	0.8937	0.84645	0.93812	0.94766	1
Model A versus model C					
Kappa location	0.99879	0.86405	0.94684	0.89461	1
Kappa histogram	0.76853	0.77863	0.89658	0.91961	1
Kappa index	0.76760	0.67278	0.84892	0.82268	1

The resume and dynamic changes of *SFS* values between models are demonstrated on Fig. 6. The highest change in classification occurs from model A to model C, from the low *SFS* on the former, to very low *SFS* on the later (23,912 cells), meaning that decreasing the role of slope angle and relative permeability results in a reduction on the *SFS* value. The same pattern is verified on the changes from very low *SFS* to "no data" (i.e., values below to 5) that can be observed in Fig. 6A by the reduction of the number of cells with very low *SFS*. The opposite situation – a change from very low to low *SFS* – is almost residual, occurring in only 144 cells from model B to model C and in 48 cells from model A to model C. An aggravation of SFS is observable from the moderate to the high class in a small number of cells, particularly from models A to B and A to C (Fig. 6B), which merits future analysis in order to understand the particular context in which such aggravation occurs.

The cartographic representation of the *SFS* scores obtained on the three models confirms the evidenced trend expressed on Fig. 6. From model A to model C, a reduction on *SFS* class and even its exclusion (for scores <5) is observed, for example, in the right-bottom corner of both Fig. 7A1 and B1 (a change of the *SFS* class from moderate to low). On the right-upper corner of Fig. 7A1 (in contrast with Fig. 7B1 and C1), a reduction from low to very low *SFS* and the elimination of small tributaries is also observed.

The visual comparison between models' results allows to conclude that model C (weighting 0.85 to F_{acc}, 0.1 to S_{avg} and 0.05 to $Prel\_inv_{avg}$) performs a filtering effect removing from the classification streams

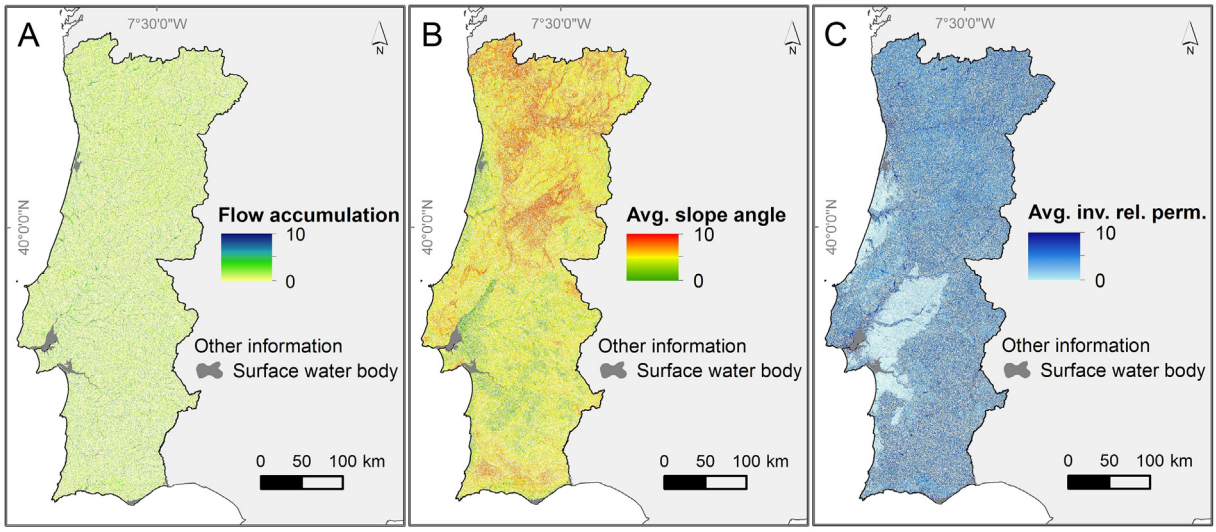

Fig. 5. Stream flood susceptibility conditioning factors: flow accumulation (A), average slope angle (B) and average inverse relative permeability (C).

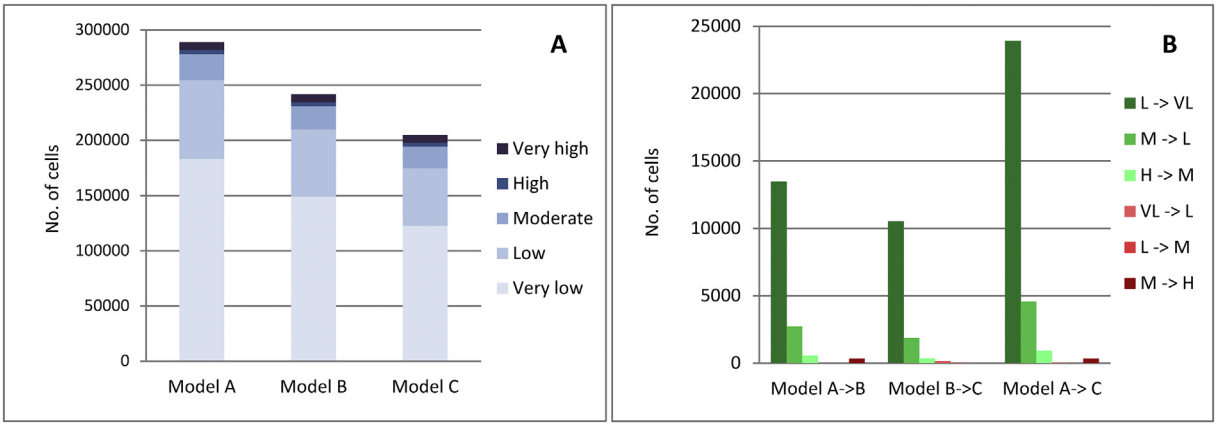

Fig. 6. Changes in stream flood susceptibility between models A, B and C: no. of cells in each SFS class (A) and no. of cells the observed a change in class (B).

that do not have a historical record of flood cases (cf. Fig. 7C1, bottom-left corner). This effect is not evident when all-type flood cases are used (Fig. 7A2, B2 and C2) since this database of flood cases (including human and material consequences) presents higher quantity and geographical dispersion in comparison to the DISASTER flood cases.

A quantification of the association between *SFS* scores and the historical flood records was performed through the calculation of the Pearson correlation coefficients (Table 4). P1 tending to −1 means that in a smaller number of cells with the highest susceptibility a higher density of flood cases is found. The opposite interpretation is valid for the correlations of type P2: positive Pearson coefficients mean that the highest densities of flood cases are associated with the highest susceptibility classes. The correlations were calculated for the three models of *SFS* in each of the validation areas — mainland Portugal (using only DISASTER flood cases), and the North, Lima River basin, Tâmega River basin and Águeda River basin (here, both DISASTER and minor flood cases were used).

Analyzing Table 4, it is observed that model C performs better than the others in three of the five validation areas regarding P1-type correlations and in two out of five regarding P2-type correlations.

The weights' combination applied in model C result in a reduction of the classified streams (cf. Fig. 6A), i.e., *SFS* scores are in general lower on model C than in the other models. This causes the elimination of streams with low susceptibility (as evidenced on Fig. 7C1) explaining the higher Pearson coefficient correlation of model C in mainland Portugal (−0.6687). In this case, the density of flood cases per cell in the higher *SFS* classes (high and very high) is higher on model C than in the other models, while the number of cells on that same *SFS* classes is lower. This results in stronger negative correlations in P1.

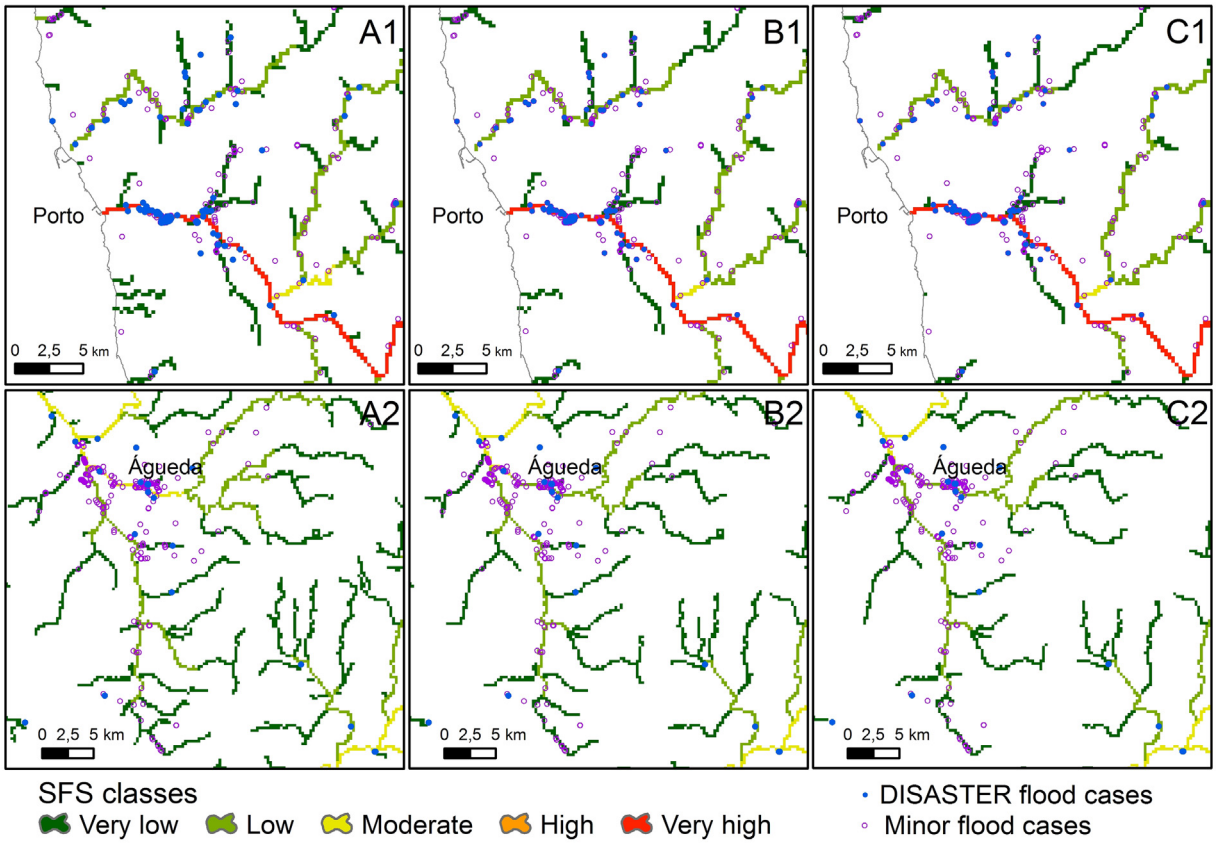

Fig. 7. Classes of *SFS* according to models A, B and C near the Douro River mouth (A1, B1 and C1) and on the Águeda River basin (A2, B2 and C2). See location of each of these plots in Fig. 3.

Table 4
Pearson correlation coefficients between validation areas and the SFS models A, B and C.

Pearson correlations	Models	Mainland Portugal	North	Lima River basin	Tâmega River basin	Águeda River basin
P1 — number of cells in each *SFS* class correlated with the number of flood cases per cell	Model A	−0.6402	−0.5962	**−0.6725**	**−0.7597**	−0.85228
	Model B	−0.6400	−0.6151	−0.5753	−0.7260	−0.90544
	Model C	**−0.6687**	**−0.6729**	−0.3845	−0.6965	**−0.99609**
P2 — class of *SFS*, from 1 (very low) to 5 (very high) correlated with the number of flood cases per cell in each SFS class	Model A	**0.9131**	0.8647	0.9482	**0.9387**	0.86278
	Model B	0.9094	0.8807	**0.9586**	0.8953	0.9315
	Model C	0.9098	**0.9249**	0.9205	0.8154	**0.99690**

Note: highest correlation coefficients in each validation area are presented in bold.

However, model A performs better than models B and C in regard to the correlation of type P2 in mainland Portugal (0.9131). Since the DISASTER database is the only one that covers the entire mainland Portugal, thus allowing a model validation to the entire study area, the decision on the best model should consider more the mainland Portugal validation area than the others. This would exclude model B. The correlation coefficients on the remaining validation areas – North, Lima, Tâmega and Águeda basins – show that model C performs slightly better than model A, and that both P1 and P2-type correlations are significantly stronger on the Águeda basin's validation area. These considerations supported the selection of model C as the best model validated according to the geographical distribution of the historical flood cases.

4.2. Municipal stream flood susceptibility

As concluded on the previous section, the *SFS* model C was chosen to evaluate the municipal *SFS* in mainland Portugal. The average value of the *SFS* scores was computed for each municipality (Fig. 8). Higher averages of *SFS* are found on municipalities crossed by transboundary rivers, particularly the Douro, Tagus and Guadiana rivers. Some coastal municipalities located at the mouth of Portuguese river basins, particularly between the Minho and the Douro rivers, are also classified on the highest *SFS* quantile (scores between 6.67 and 8.86). The lower classes of average *SFS* by municipality – e.g. the lowest six quantiles – express local differences that should be

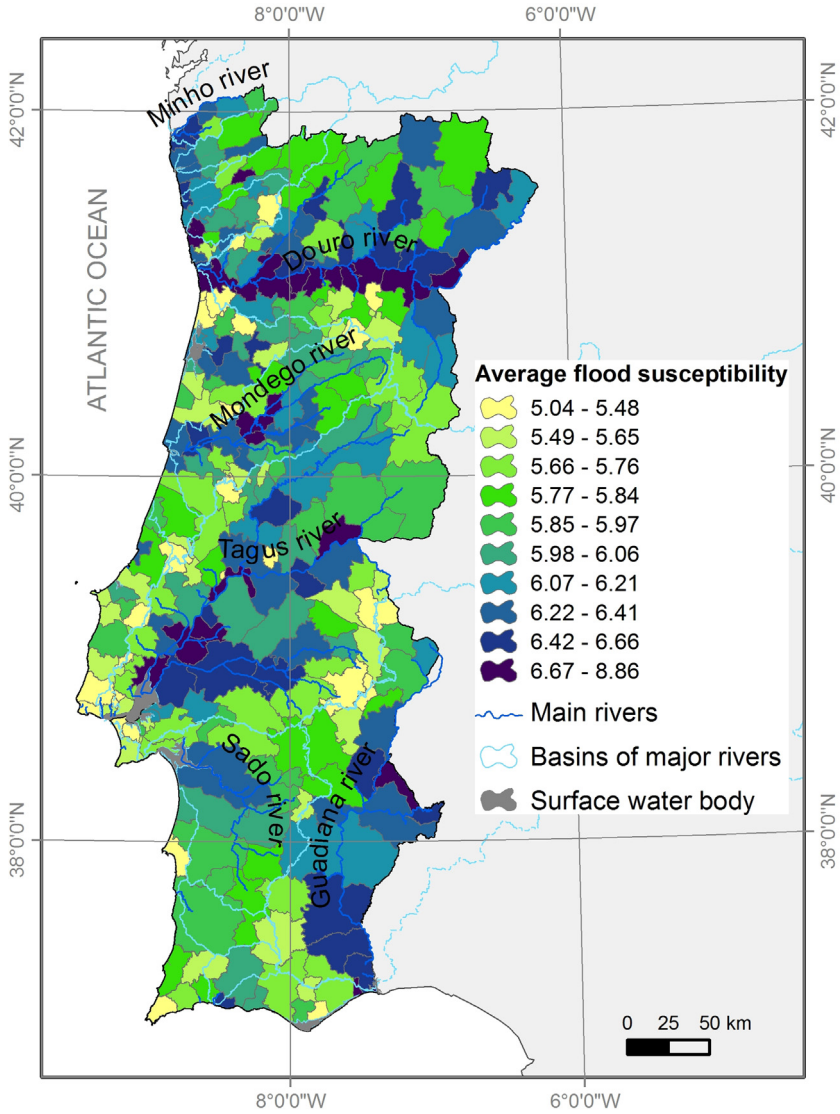

Fig. 8. Average flood susceptibility by municipality, according to *SFS* obtained from model C. Classification in 10 classes of equal number of individuals (quantiles).

further analyzed taking into account the local hydrologic and geomorphologic characteristics of the respective watersheds.

The DISASTER flood cases can be included on a cross-analysis with the average *SFS* by municipality because the source database covers the entire territory of mainland Portugal in a systematic process. A scatter-plot between the two variables (Fig. 9) represents the geographical particularities of susceptibility and past flood disasters, contributing to the definition of the municipal profiles of flood risk. Fig. 9 shows that there are territorial contexts of flood losses where it should not be expected considering the average *SFS* (exemplified by Loures, Oeiras, Sintra and Odivelas municipalities), as well as there are contexts of high *SFS* with absence or a small number of DISASTER cases (exemplified by Mourão or V.R.S. António municipalities).

The record of DISASTER flood cases by municipality was classified in 4 classes and crossed with the classes of municipal average *SFS* as a 2-entry matrix, as presented on Table 5.

The 2-entry matrix defines 5 profiles of municipalities, described in Table 5, ranging from the safest A profile – with absence of DISASTER flood cases and *SFS* classes of very low and low – to the most severe profile E with 10 or more cases and *SFS* classes of moderate, high and very high (cf. with Fig. 10). Results show that there are 7 municipalities with low average *SFS* but presenting a high number of DISASTER flood cases (4 municipalities with 10 to 19 cases and 3 municipalities with >20 cases), which should deserve a major concern from policy makers and risk practitioners as they express situations of high exposure and/or high vulnerability. It should be reminded that DISASTER cases demand the record of one or more casualties, missing, injured, displaced or evacuated persons. In the opposite context, it is noted that two municipalities are classified with moderate and high average *SFS* on model C but they do not register DISASTER flood cases. The territorial factors that justify such flood safety on the two municipalities are also relevant for flood risk management.

5. Discussion

5.1. Advantages and disadvantages of the SFS methodological approach

The use of multicriteria approaches to assess flood susceptibility is widely disseminated because of a) the new computational possibilities enables the use of diverse geographical datasets and training algorithms and b) their ability to produce cost-effective cartography to large areas (regional and national scales) and simultaneously maintaining the consistency and spatial homogeneity of the method's application.

A wide range of flood conditioning factors can be used for stream flood susceptibility assessment. The *SFS* approach used three factors applying them the same cumulative and average functions. Eventually, the use of other factors would evidence a significant redundancy as most of the factors depend either on flow accumulation (basin's area and river hierarchy, among others) or on permeability (i.e., drainage density, land use or rainfall-runoff ratio).

It should be noted that there is not a standard and universal weighting that might be applied to all the study areas or basins. The results herein presented showed that the best combination of flood conditioning factors for mainland Portugal was not the one that best performed on some of the basins where validation was conducted.

All the flood conditioning factors are considered to be constant in time, with the exception of land use from the CLC2012. Quite often, the use of long historical flood databases along with the use of current datasets expressing land use characteristics is pointed out as a weakness to models because the past flood events' conditions might not correspond to the current conditions. If this is partly correct, one cannot ignore too that the presented method represents a natural susceptibility to flooding, in which land use is applied only as a component that influences the natural permeability evaluated from parent dominant material and the fine fraction of the topsoil. Relative permeability is also the factor that receives the smallest weight. Moreover, the *SFS* scores express a long-term predisposition to flooding.

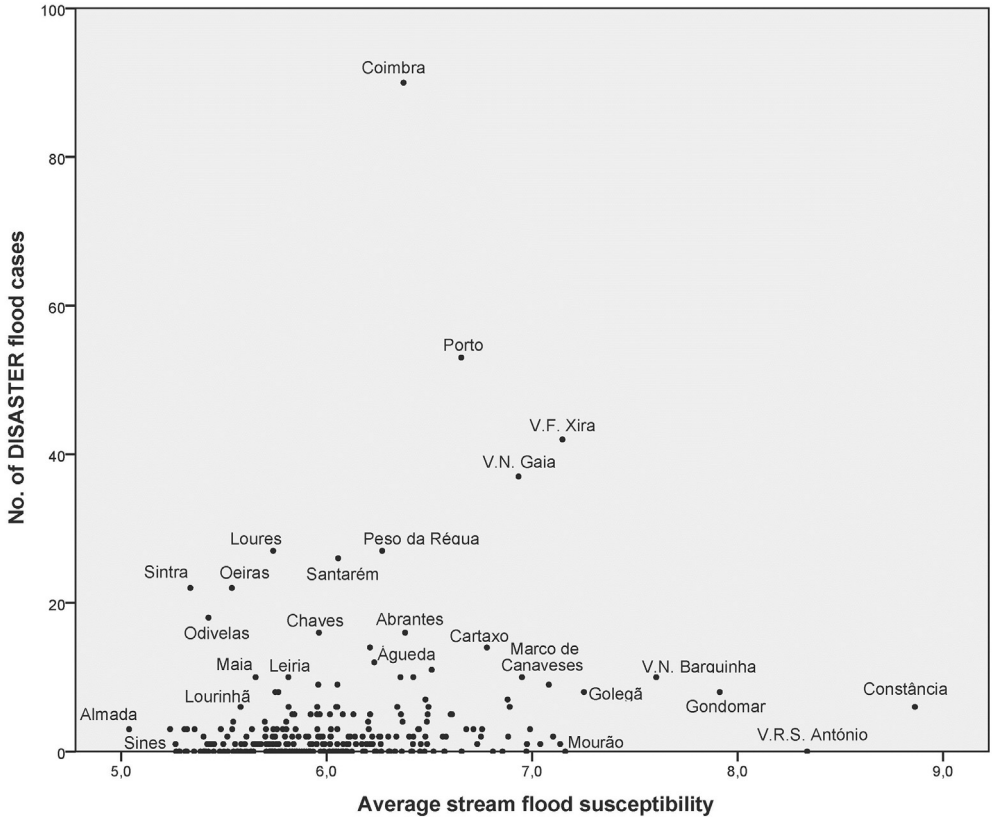

Fig. 9. Average *SFS* per municipality and the number of DISASTER flood cases.

Table 5
Classes of average *SFS* per municipality and classes of DISASTER cases per municipality. Colors identify municipal profiles of flood risk: profile A (dark green), profile B (light green), profile C (orange), profile D (light red) and profile E (dark red).

Classes of average *SFS* per municipality	Classes of DISASTER flood cases per municipality				
	1 — 0 cases	2 — 1 to 9 cases	3 — 10 to 19 cases	4 — 20 to 90 cases	No. of municipalities
Very low [5.24, 6]	64	78	4	3	*149*
Low [6, 7]	39	66	8	5	*118*
Moderate [7, 8]	1	6	1	1	*9*
High [8, 9]	1	1	0	0	*2*
Very high [9, 10]	0	0	0	0	*0*
No. of municipalities	*105*	*151*	*13*	*9*	*278*

Another issue regarding databases of historical flood cases and its use to validate susceptibility models is that the geographical distribution of flood cases is strongly influenced by the location and exposure of human settlements to river flooding, causing a higher concentration of flood cases near to streams that are not necessarily the more susceptible to generate flooding. The low coverage of such databases in more remote areas must be considered.

Susceptibility assessments which intent the definition of flood-prone areas encounter an additional challenge in using historical flood records for validation: very often, flooded areas in the low probability

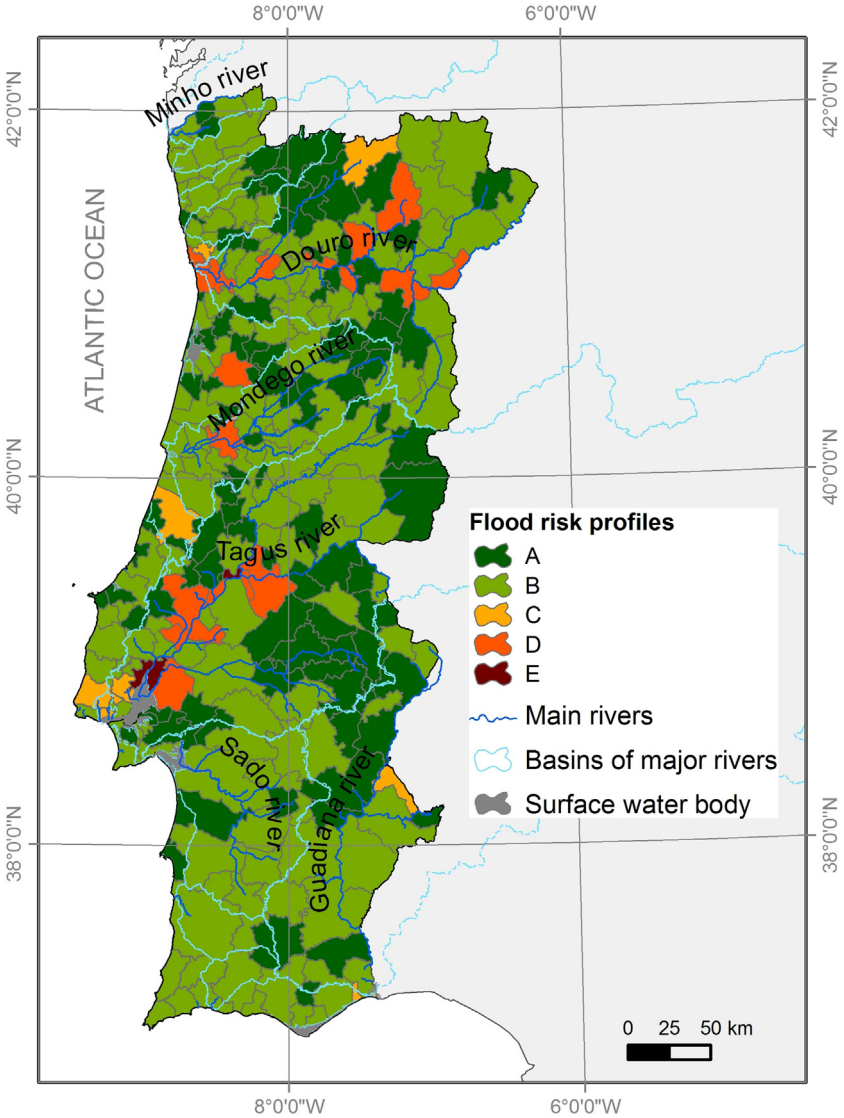

Fig. 10. Municipal flood risk profiles.

events are located at the border of floodplains, where the data recorded on a given cell may already be expressing the context of the basis of the slope (higher slopes, non-alluvial soils, etc.), thus inducing in error the assignment of weights to the conditioning factors. The *SFS* approach does not suffer from this drawback since flood locations – whether located on the streamline whether located at the border of the floodplain – are accounted for validating the susceptibility of that same streamline.

However in the presented study, it was not possible to use validation areas from the southern region of mainland Portugal due to the lack of an inventory of flood cases with only material consequences (like it was possible to be done on the Lima, Tâmega and Águeda basins as well as on the North region). This implied that the evaluated correlations were expressing only specific geographical contexts found on the northern and central regions of mainland Portugal.

5.2. Applications of SFS knowledge in flood risk management

The cell-by-cell assessment of *SFS* and the aggregated municipal risk profiles have distinct applications in flood risk management.

The municipal flood risk profiles identify the contexts of flood susceptibility and losses in support of strategic decision-making in flood risk management. The following five profiles were defined (Fig. 10):

- Profile A: the group of 103 municipalities on this profile represents the safest context in terms of flood risk, this means, low *SFS* coinciding with the absence of DISASTER flood cases. Predominately hilltop-municipalities or coastal lowland municipalities with local streams constitute the majority of municipalities with this profile, as Sines (cf. Fig. 8);
- Profile B: the 144 municipalities of this profile present the same *SFS* conditions and a minor report of flood cases (1 to 9), such as Lourinhã (6 cases) or Almada (3 cases), explained more by the exposure conditions than by the natural flooding predisposition;
- Profile C: this group only includes 9 municipalities, however, with two distinct contexts: one with moderate and high *SFS* but no DISASTER flood cases (Mourão and V.R.S. António, respectively) and other in which the urban sprawl and exposure are responsible for the high number of cases (10 or more), regardless of a very low *SFS* (for example, Oeiras, Odivelas, Loures, Chaves or Maia) (cf. Fig. 9 and Fig. 10);
- Profile D: excluding profile E, the profile D represents the more concerning susceptibility and losses contexts. Two groups are present: a group of 13 with low *SFS* if the national scale is considered (average *SFS* ≥ 6 and < 7) but with 10 or more flood cases (this first group is heterogeneous and includes municipalities from Portuguese and international basins, such as Águeda, Cartaxo, Santarém, Porto or Coimbra); a second group of 7 municipalities, all associated whether to the Douro basin (e.g. Gondomar) or to the Tagus basin (e.g. Constância, and Golegã), with moderate and high *SFS* but only 1 to 9 flood cases;
- Profile E: the two municipalities of this profile (V.N. Barquinha and V.F. Xira) partly occupy the Tagus floodplain although the average *SFS* is only of 7,6 and 7,2, respectively (moderate *SFS*), but they present a historical record of disastrous floods (particularly V.F. Xira with 42 flood cases).

The cell-by-cell results are valuable in other, more detailed, applications in flood risk management. When crossed with historical records and exposure data, the *SFS* results have the ability to identify priority reaches of the river network to benefit from early warning systems, additional land use regulations, local engineering mitigation structures and have the ability to be applied in support of urban development plans (e.g. Bathrellos et al., 2017) and multi-level integrated spatial planning systems (e.g. Ran and Nedovic-Budic, 2016). The SFS data can be used in the production of comparable results for basins with similar areas; the modeling of permeability condition changes – caused, for example, by land use changes – and its effect on *SFS*; the identification of naturally priority areas of higher susceptibility for the application of hydrologic and hydraulic (1D or 2D) modeling at the local scale.

6. Conclusions

The presented methodology assesses the predisposing flood conditions at the national scale based on three types of data: flow accumulation, slope angle and relative permeability. Validation through the correlation of susceptibility with historical records highlights the relevance of the existence of long flood databases, independently of the dynamics of exposure and land use. Regardless the limitations on the use of historical flood databases in method's validation, it proved to be undoubtedly useful on the understanding of fluvial and exposure geographical contexts in which flood losses take place, when analyzed along with flood susceptibility data, and producing municipal profiles of flood risk.

These are the main achievements of this research:

- The definition of a methodology which provides a comparable nation-wide evaluation of streams' susceptibility to flooding, incorporating data from the entire contributive areas and not only from the on-site characteristics of streams.
- The identification of areas of natural susceptibility not conditioned by the existence of a historical record of losses, often biased by exposure and vulnerability. In fact, in a preventive logic of risk management, it is not only important to consider the areas with an historical record of flood losses — like it is done in the implementation of the Flood's Directive, as also to prevent the urban development in the more susceptible areas.
- The definition of a municipal index which allows to rank and to identify the administrative units with higher priority for the allocation of prevention and mitigation resources – like flood monitoring and early warning systems – as well as for an adequate emergency response according to the predominant type of impacts.

The future research includes the use of the cumulative function in a wider set of factors – drainage density, elevation, land use, rainfall and other morphological or hydrographical indexes. If applied to basins – not administrative areas – of similar area, the methodological approach will be able to isolate to role of each factor in defining the stream's flood susceptibility. Ultimately, such factors are related to the factors applied on the presented study, although this too requires testing.

Another aspect to consider in future research is the application of the *SFS* methodology to help respond to the question of where is more probable to testify the beginning of river overbanking, this means, the starting point of flooding along a streamline. In fact, most methods identify the areas to which a flood may accumulate and expand. The *SFS* approach has the ability to differentiate streams with the same contributing area, based on other conditioning factors which may be correlated to the floodplain's morphology.

Acknowledgements

This work was financed by national funds through FCT — Portuguese Foundation for Science and Technology, I.P., under the framework of the project FORLAND – Hydro-geomorphologic risk in Portugal: driving forces and application for land use planning (PTDC/ATPGEO/1660/2014) and by the Research Unit UID/GEO/00295/2019.

References

Ballabio, C., Panagos, P., Monatanarella, L., 2016. Mapping topsoil physical properties at European scale using the LUCAS database. Geoderma 261, 110–123. https://doi.org/10.1016/j.geoderma.2015.07.006.

Bathrellos, G.D., Skilodimou, H.D., Chousianitis, K., Youssef, A.M., Pradhan, B., 2017. Suitability estimation for urban development using multi-hazard assessment map. Sci. Total Environ. 575, 119–134. https://doi.org/10.1016/J.SCITOTENV.2016.10.025.

Benito, G., Lang, M., Barriendos, M., Llasat, C., Francés, F., Ouarda, T., Varyl, R., Enzel, Y., Bardossy, A., 2004. Use of systematic, palaeoflood and historical data for the improvement of flood risk estimation. Review of scientific methods. Nat. Hazards 31, 623–643. https://doi.org/10.1023/B:NHAZ.0000024895.48463.eb.

Casas, A., Benito, G., Thorndycraft, V.R., Rico, M., 2006. The topographic data source of digital terrain models as a key element in the accuracy of hydraulic flood modelling. Earth Surf. Process. Landf. 31, 444–456. https://doi.org/10.1002/esp.1278.

Cohen, J., 1960. A coefficient of agreement for nominal scales. Educ. Psychol. Meas. XX, pp. 37–46.

Cunha, N.S., Magalhães, M.R., Domingos, T., Abreu, M.M., Küpfer, C., 2017. The land morphology approach to flood risk mapping: an application to Portugal. J. Environ. Manag. 193, 172–187. https://doi.org/10.1016/j.jenvman.2017.01.077.

Diéz-Herrero, A., Benito, G., Bodoque, J.M., 2013. Las avenidas e inundaciones históricas del Tajo en Toledo. In: Iribas, B.L., Saavedra, A.C. (Eds.), El Río Tajo, Lecciones Del Passado Para Un Futuro Mejor. Toledo.

EEA, 2012. CORINE Land Cover 2012 (CLC2012).

Gallego, M.C., Trigo, R.M., Vaquero, J.M., Brunet, M., García, J.A., Sigró, J., Valente, M.A., 2011. Trends in frequency indices of daily precipitation over the Iberian Peninsula during the last century. J. Geophys. Res. 116, D02109. https://doi.org/10.1029/2010JD014255.

Garrote, J., Díez-Herrero, A., Bodoque, J., Perucha, M., Mayer, P., Génova, M., 2017. Flood hazard management in public mountain recreation areas vs. ungauged fluvial basins. Case study of the Caldera de Taburiente National Park, Canary Islands (Spain). Geosciences 8, 6. https://doi.org/10.3390/geosciences8010006.

Hagen, E., Shroder, J.F., Lu, X.X., Teufert, J.F., 2010. Reverse engineered flood hazard mapping in Afghanistan: a parsimonious flood map model for developing countries. Quat. Int. 226, 82–91. https://doi.org/10.1016/j.quaint.2009.11.021.

Hong, H., Panahi, M., Shirzadi, A., Ma, T., Liu, J., Zhu, A.X., Chen, W., Kougias, I., Kazakis, N., 2018. Flood susceptibility assessment in Hengfeng area coupling adaptive neuro-fuzzy inference system with genetic algorithm and differential evolution. Sci. Total Environ. 621, 1124–1141. https://doi.org/10.1016/j.scitotenv.2017.10.114.

Jacinto, R., Grosso, N., Reis, E., Dias, L., Santos, F.D., Garrett, P., 2015. Continental Portuguese territory flood susceptibility index – contribution to a vulnerability index. Nat. Hazards Earth Syst. Sci. 15, 1907–1919. https://doi.org/10.5194/nhess-15-1907-2015.

Kazakis, N., Kougias, I., Patsialis, T., 2015. Assessment of flood hazard areas at a regional scale using an index-based approach and analytical hierarchy process: application in Rhodope-Evros region, Greece. Sci. Total Environ. 538, 555–563. https://doi.org/10.1016/j.scitotenv.2015.08.055.

Kourgialas, N.N., Karatzas, G.P., 2011. Flood management and a GIS modelling method to assess flood-hazard areas—a case study. Hydrol. Sci. J. 56, 212–225. https://doi.org/10.1080/02626667.2011.555836.

Kourgialas, N.N., Karatzas, G.P., 2017. A national scale flood hazard mapping methodology: the case of Greece — protection and adaptation policy approaches. Sci. Total Environ. 601–602, 441–452. https://doi.org/10.1016/J.SCITOTENV.2017.05.197.

Landis, J.R., Koch, G.G., 1977. The measurement of observer agreement for categorical data. Biometrics 33, 159–174. https://doi.org/http://www.jstor.org/stable/2529310.

Lee, M.-J., Kang, J.-E., Jeon, S., 2012. Application of frequency ratio model and validation for predictive flooded area susceptibility mapping using GIS. Geoscience and Remote Sensing Symposium (IGARSS 2012). IEEE, Munich, pp. 895–898.

de Lima, M.I.P., Santo, F.E., Ramos, A.M., Trigo, R.M., 2015. Trends and correlations in annual extreme precipitation indices for mainland Portugal, 1941–2007. Theor. Appl. Climatol. 119, 55–75. https://doi.org/10.1007/s00704-013-1079-6.

Manfreda, S., Nardi, F., Samela, C., Grimaldi, S., Taramasso, A.C., Roth, G., Sole, A., 2014. Investigation on the use of geomorphic approaches for the delineation of flood prone areas. J. Hydrol. 517, 863–876. https://doi.org/10.1016/j.jhydrol.2014.06.009.

Miranda, P.M.A., Coelho, F.E.S., Tomé, A.R., Valente, M.A., Pires, H.O., Pires, V.C., Ramalho, C., 2002. 20th century Portuguese climate and climate scenarios. In: Santos, F., Forbes, K., Moita, R. (Eds.), Climate Change in Portugal: Scenarios, Impacts and Adaptation Measures. Gradiva, pp. 27–83.

Panagos, P., Van Liedekerke, M., Jones, A., Montanarella, L., 2012. European Soil Data Centre: response to European policy support and public data requirements. Land Use Policy 29, 329–338. https://doi.org/10.1016/j.landusepol.2011.07.003.

Pradhan, B., 2009. Flood susceptible mapping and risk area delineation using logistic regression. GIS and remote sensing. Journal of Spatial Hydrology 9 (2), 1–18.

Rahmati, O., Pourghasemi, H.R., Zeinivand, H., 2016. Flood susceptibility mapping using frequency ratio and weights-of-evidence models in the Golastan Province, Iran. Geocarto Int. 31 (1), 42–70. https://doi.org/10.1080/10106049.2015.1041559.

Ramos, A.M., Cortesi, N., Trigo, R.M., 2014. Circulation weather types and spatial variability of daily precipitation in the Iberian Peninsula. Front. Earth Sci. 2, 1–17. https://doi.org/10.3389/feart.2014.00025.

Ran, J., Nedovic-Budic, Z., 2016. Integrating spatial planning and flood risk management: a new conceptual framework for the spatially integrated policy infrastructure. Comput. Environ. Urban. Syst. 57, 68–79. https://doi.org/10.1016/J.COMPENVURBSYS.2016.01.008.

Razavi Termeh, S.V., Kornejady, A., Pourghasemi, H.R., Keesstra, S., 2018. Flood susceptibility mapping using novel ensembles of adaptive neuro fuzzy inference system and metaheuristic algorithms. Sci. Total Environ. 615, 438–451. https://doi.org/10.1016/j.scitotenv.2017.09.262.

Reis, E., 2011. Análise de bacias hidrográficas, susceptibilidade à ocorrências de cheias e sistemas de informaçao geográfica: da definiçao do quadro conceptual até à proposta de um modelo de avaliação. VIII Congresso Da Geografia Portuguesa. Associaçao Portuguesa de Geógrafos, Lisboa, pp. 1–6.

Saksena, S., Merwade, V., 2015. Incorporating the effect of DEM resolution and accuracy for improved flood inundation mapping. J. Hydrol. 530, 180–194. https://doi.org/10.1016/j.jhydrol.2015.09.069.

Santos, M., Fragoso, M., Santos, J.A., 2018. Damaging flood severity assessment in northern Portugal over more than 150 years (1865-2016). Nat. Hazards https://doi.org/10.1007/s11069-017-3166-y.

Santos, P.P., Reis, E., 2018. Assessment of stream flood susceptibility: a cross-analysis between model results and flood losses. J. Flood Risk Manage. 11. https://doi.org/10.1111/jfr3.12290.

Santos, P.P., Tavares, A.O., Andrade, A.I.A.S.S., 2011. Comparing historical-hydrogeomorphological reconstitution and hydrological-hydraulic modelling in the estimation of flood-prone areas—a case study in Central Portugal. Nat. Hazards Earth Syst. Sci. 11, 1669–1681. https://doi.org/10.5194/nhess-11-1669-2011.

Tehrany, M.S., Pradhan, B., Jebur, M.N., 2014. Flood susceptibility mapping using a novel ensemble weights-of-evidence and support vector machine models in GIS. J. Hydrol. 512, 332–343. https://doi.org/10.1016/j.jhydrol.2014.03.008.

Tehrany, M.S., Pradhan, B., Mansor, S., Ahmad, N., 2015. Flood susceptibility assessment using GIS-based support vector machine model with different kernel types. Catena 125, 91–101. https://doi.org/10.1016/j.catena.2014.10.017.

Trigo, R.M., Dacamara, C.C., 2000. Circulation weather types and their influence on the precipitation regime in Portugal. Int. J. Climatol. 20 (13), 1559–1581. https://doi.org/10.1002/1097-0088(20001115)20:13<1559::AID-JOC555>3.0.CO;2-5.

Vahid, S., Termeh, R., Kornejady, A., Reza, H., Keesstra, S., 2018. Flood susceptibility mapping using novel ensembles of adaptive neuro fuzzy inference system and metaheuristic algorithms. Sci. Total Environ. 615, 438–451. https://doi.org/10.1016/j.scitotenv.2017.09.262.

Visser, H., De Nijs, T., 2006. The map comparison kit. Environ. Model. Softw. 21, 346–358. https://doi.org/10.1016/j.envsoft.2004.11.013.

Vojtek, M., Vojteková, J., 2016. Flood hazard and flood risk assessment at the local spatial scale: a case study. Geomat. Nat. Haz. Risk 7, 1973–1992. https://doi.org/10.1080/19475705.2016.1166874.

Wing, O.E.J., Bates, P.D., Smith, A.M., Sampson, C.C., Johnson, K.A., Fargione, J., Morefield, P., 2018. Estimates of present and future flood risk in the conterminous United States. Environ. Res. Lett. 13. https://doi.org/10.1088/1748-9326/aaac65.

Yang, X.L., Ding, J.H., Hou, H., 2013. Application of a triangular fuzzy AHP approach for flood risk evaluation and response measures analysis. Nat. Hazards 68, 657–674. https://doi.org/10.1007/s11069-013-0642-x.

Zêzere, J.L., Pereira, S., Tavares, A.O., Bateira, C., Trigo, R.M., Quaresma, I., Santos, P.P., Santos, M., Verde, J., 2014. DISASTER: a GIS database on hydro-geomorphologic disasters in Portugal. Nat. Hazards 72, 503–532. https://doi.org/10.1007/s11069-013-1018-y.

Zhao, G., Pang, B., Xu, Z., Yue, J., Tu, T., 2018. Mapping flood susceptibility in mountainous areas on a national scale in China. Sci. Total Environ. 615, 1133–1142. https://doi.org/10.1016/J.SCITOTENV.2017.10.037.